ACS Macro Letters

Letter

pubs.acs.org/macroletters

The Effect of Surface Chemistry on the Glass Transition of Polycarbonate Inside Cylindrical Nanopores

Dariya K. Reid,[†] Marcela Alves Freire,[‡] Haiqing Yao,[§] Hung-Jue Sue,[§,∥] and Jodie L. Lutkenhaus*[,†,§]

[†]Artie McFerrin Department of Chemical Engineering, [§]Department of Materials Science and Engineering, and [∥]Polymer Technology Center, Department of Mechanical Engineering, Texas A&M University, College Station, Texas 77843, United States

[‡]Universidade Federal de Minas Gerais, Pampulha, Belo Horizonte, MG 31270-901, Brazil

Supporting Information

ABSTRACT: The effect of surface chemistry on the glass transition of polycarbonate (PC) inside cylindrical nanopores is studied. Polycarbonate is melt-wetted into nanoporous anodic aluminum oxide (AAO) treated with hydrophobic alkyl- and fluorosilanes of varying length. The curvature observed at the nanowire tips is consistent with a contact angle descriptive of polycarbonate−AAO surface interactions. Differential scanning calorimetry (DSC) thermograms reveal a distinct broadening of the T_g that is related to the motion of polymer chains at the nanopore wall as well as at the core. DSC and thermal gravimetric analysis (TGA) show that polycarbonate infiltrated into a naked AAO template (without silane treatment) degrades upon heating, suggestive of a surface-catalyzed degradation mechanism. It is further shown that silane treatment largely prevents PC thermal degradation.

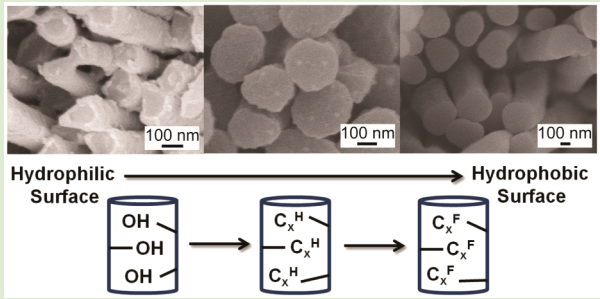

The effect of confinement on the glass transition temperature (T_g) remains a topic of intense discussion. As a polymer film decreases in thickness, the effect of the surface grows in dominance, and the films' properties differ from bulk. The nature of the supporting surface can drastically alter the T_g for amorphous polymer thin films. For instance, free-standing poly(styrene) films showed a greater reduction in T_g as compared to films deposited on hydrogen-passivated Si(111).[1] Elsewhere, the T_g of poly(styrene) thin films decreased or increased depending on whether the supporting surface was repulsive or attractive, respectively.[2]

In this work we report the effect of surface chemistry on interactions between polycarbonate (PC) and nanoporous silane-modified anodic aluminum oxide (AAO) templates as well as the resulting changes in the glass transition of the polymer (Figure 1). This configuration is convenient for isolating the effect of surface chemistry because AAO templates are easily modified via silanes and because the infiltrated polymer has negligible free surface. Modification of AAO templates using silane chemistry has been previously demonstrated using both vapor-phase[3−6] and solution approaches.[7−11]

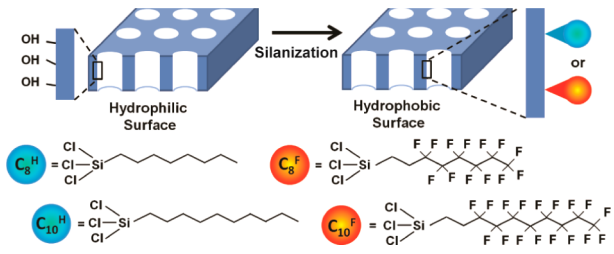

Figure 1. Schematic representation of functionalization of nanoporous AAO templates.

PC, popularly used in many industrial applications, is a semicrystalline polymer. The reported melting temperature (T_m) and T_g is 220−260 °C and 140−151 °C, respectively.[12] Crystallization of PC is slow, occurring on the order of days and weeks.[13] For the purposes of this investigation, the experimental conditions are manipulated such that only the amorphous phase is observed.

Significant effort has been made to study the segmental dynamics of polymers confined in AAO pores.[14−17] Serghei et al. found no alteration in poly-2-vinylpyridine chain dynamics in pores as small as 18 nm in diameter.[17] On the other hand, Duran et al. observed slower dynamics for AAO-confined polypeptides.[15] Krutyeva et al. proposed dual-mode dynamics attributed to an anchored surface layer separate from bulk for poly(dimethylsiloxane) inside AAO pores 26 nm in diameter.[16] Blaszczyk-Lezak et al. reported highly constrained relaxation of poly(methyl methacrylate) (PMMA) at the surface of the AAO pores 28 nm in diameter.[14]

AAO templates possess a local environment similar to that of controlled pore glasses (CPGs), for which there have been numerous reports on the effects of confinement of glass formers.[18−23] For instance, two distinct T_g's were observed for

Received: November 13, 2014
Accepted: January 5, 2015
Published: January 13, 2015

DOI: 10.1021/mz500725s
ACS Macro Lett. 2015, 4, 151−154

4-cumylphenol cyanate ester[18] and bisphenol M dicyanate ester[20] confined inside CPGs. Primary and secondary T_g's were associated with the material at the center and surface of the pores, respectively.[20] Researchers also observed that both T_g's shifted to lower temperatures as the pore diameter decreased. Similarly, a reduction in T_g and T_m with increased confinement was observed for a series of organic liquids.[21−23] Elsewhere, Shin et al. observed a broadening in the T_g of AAO-confined poly(styrene) but no distinctive shift in absolute value.[24] Recently Li et al. presented work on the effect of cooling conditions on the glass transition of PMMA inside cylindrical nanopores. Upon fast cooling a single T_g was detected, while slow cooling resulted in two T_g's.[25]

To our knowledge, there exists a lack of knowledge on the effect of surface chemistry on the T_g of the cylindrically confined amorphous polymer. On the other hand, silane-modified AAO membranes have been previously used to study the effect of confinement on polymer crystallization.[26] Confined syndiotactic polystyrene (sPS) exhibited an increase in crystallinity as the crystallization temperature decreased, whereas the crystallinity of bulk sPS remained constant. In addition, crystallization of sPS confined inside AAO passivated with *n*-hexyltrimethoxysilane was suppressed as compared to sPS crystallized inside pristine AAO.[26] These results with semicrystalline polymer suggest that the surface may similarly influence the glass transition of amorphous PC.

PC was melt-pressed into nanoporous AAO templates of 200 nm pore diameter. Native, unmodified AAO templates were compared to those modified with a series of silanes to study the effect of chain length and chain composition: (tridecafluoro-1,1,2,2-tetrahydrooctyl)trichlorosilane ($C_8H_4F_{13}Cl_3Si$, "C^F_8"), (heptadecafluoro-1,1,2,2-tetrahydrodecyl)trichlorosilane ($C_{10}H_4F_{17}Cl_3Si$, "C^F_{10}"), *n*-octyltrichlorosilane ($C_8H_{17}Cl_3Si$, "C^H_8"), *n*-decyltrichlorosilane ($C_{10}H_{21}Cl_3Si$, "C^H_{10}") (Figure 1). A detailed description of the preparation is provided in the Supporting Information.

Attempts to infiltrate PC into templates with smaller pore diameters (40 and 15 nm) proved unsuccessful because of the slow rate of infiltration. The rate of polymer infiltration into nanopores has been previously expressed as follows[27]

$$dz/dt = (R\gamma \cos(\theta_c))/4\eta z \quad (1)$$

where t is time; z is the depth of polymer melt infiltration; η is polymer melt viscosity; R is hydraulic radius; θ_c is contact angle; and γ is surface tension. Accordingly, as pore diameter decreases, so does the rate of infiltration. This slow rate may also be attributed to the high viscosity of the PC melt. To promote infiltration, increased pressures and temperatures were explored, but both resulted in yellowing of the sample. For these reasons, we selected melt-pressing of PC for 8 h at 232 °C under 0.25 Torr of pressure as an optimum for the 200 nm diameter porous templates.

Figure 2 shows PC nanowires prepared by melt-pressing after selective removal of the template. Nanowires prepared from bare AAO (Figure 2(a)) exhibited cupped tips, reflective of the θ_c between PC and the pore wall. The cupping is consistent with a low θ_c and is suggestive of favorable interactions between the polymer melt and the nanopore surface. Further, the nanowire diameter is comparable to the diameter of the original template. Nanowires obtained from alkyl- and fluoro-silanized AAO templates also exhibit similar diameters of about 200 nm (Figure 2(b)), but the tips for the nanowires from the fluorosilane samples are remarkably flat (Figure 2(d,f)). The

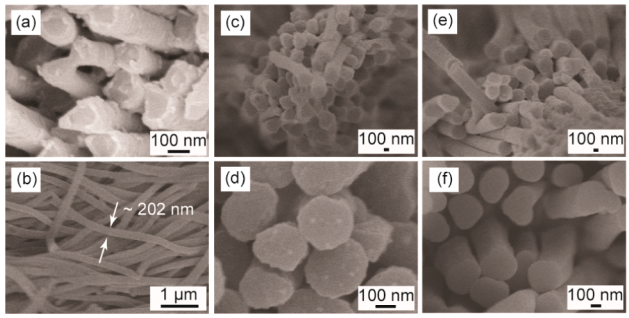

Figure 2. Scanning electron microscope (SEM) images of the released PC nanowires; structures prepared from (a) untreated AAO templates and AAO templates silanized using (b) C^H_8, (c) C^H_8, (d) C^F_8, (e) C^H_{10}, and (f) C^F_{10}.

flat nanowire tips are consistent with a relatively higher θ_c and are indicative of less favorable interactions between the PC and silane-treated wall, as compared to the native AAO. In comparison, the alkylsilane-modified AAO yielded PC nanowires (Figure 2(c,e)) with tips intermediate to that of bulk and fluorosilane samples.

PC-infiltrated AAO templates were analyzed using modulated differential scanning calorimetry (DSC) to identify the glass transition and other thermal features. Excess polymer was removed from the template's surface prior to the measurement. Modulated DSC proved necessary because the T_g was weak and overlapped with physical aging. Figure 3 and Figure S1

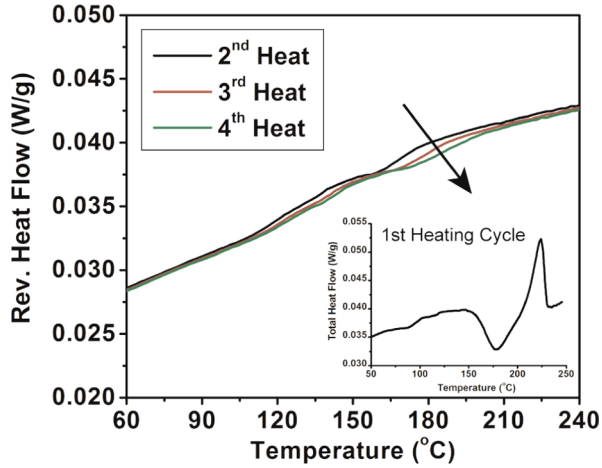

Figure 3. Reversing heat flow of PC infiltrated into untreated AAO templates for the second through fourth heating cycles. The arrow indicates the shift in the T_g. The inset shows the total heat flow from the first heating cycles. Data were obtained using modulated DSC at a scan rate, amplitude, and period of 2 °C/min, 1.272 °C, and 60 s, respectively.

(Supporting Information) show consecutive heating scans for PC infiltrated into a native AAO template. The first heating scan shows evidence of cold crystallization and melting at 177.4 and 224.0 °C, respectively. Subsequent heating scans are devoid of crystallization and exhibit a T_g that drifts toward higher temperatures with each successive scan. Because of the drift, a reliable assignment of the T_g proved untenable. The drift in T_g is likely due to degradation of the polymer or its reaction with hydroxyl groups on the nanopore's surface. This is consistent with our prior observation that native AAO can catalyze reactions with the infiltrated polymer.[28] Further, the sample in

DOI: 10.1021/mz500725s
ACS Macro Lett. 2015, 4, 151−154

native AAO showed distinctive yellowing following melt-pressing, which is suggestive of degradation. Other studies have shown a drift in the thermal transition temperatures of poly(trimethylene malonate)[29] and electrospun chitosan-gelatin nanofibers[30] due to degradation using DSC.

The thermal properties of PC infiltrated into silanized AAO templates were compared to that of bulk (Figure 4 and Figure S2, Supporting Information). Silanization appeared to arrest degradation in that little to no drift in the T_g or yellowing of the sample was observed. This result supports the hypothesis that the native AAO surface participates in PC degradation. The position and shape of the glass transition for PC in the silanized templates largely resembled that of bulk PC with the exception that the glass transition for the confined samples appeared to overlap with a second feature at slightly higher temperatures. The secondary feature observed herein for the confined PC is suggestive of a second overlapping T_g, although it is difficult to resolve. These results are similar to previous studies of bisphenol M dicyanate ester[20] and tris(4-cumylphenol)-1,3,5-triazine[31] confined inside CPGs, where two distinct T_g's were reported. One T_g was related to the material at the center of the pore, and a second higher T_g was related to the material at the pore surface. It is also possible that the secondary feature is simply a broadening of the T_g brought about by slower dynamics caused by interfacial effects.

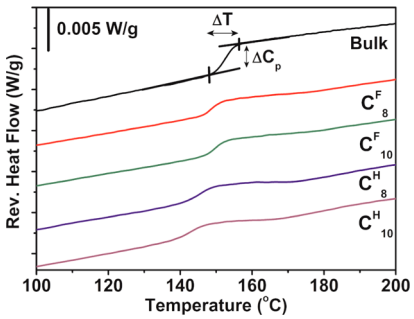

Figure 4. Modulated DSC heating scans for bulk PC and PC-infiltrated into silanized AAO templates. The second scan is presented with the exotherm oriented down. Scan rate, amplitude, and period for confined samples were 2 °C/min, 1.272 °C, and 60 s, respectively. Scan rate, amplitude, and period for bulk samples were 1 °C/min, 0.159 °C, and 40 s, respectively.

Thermal gravimetric analysis (TGA) was employed to determine the mass of PC melt-pressed into the nanoporous AAO templates of varying surface chemistry (Table 1). For this purpose, samples were prepared using conditions identical to DSC preparation. The percent weight loss was monitored as the samples were heated to 800 °C under nitrogen (Figure S3, Supporting Information). Onset temperature (T_o) denotes the beginning of weight loss. Samples prepared from untreated AAO exhibited a higher mass loss (34.1 wt %) and lower T_o (243 °C), likely due to PC degradation. No clear trend was observed among the samples prepared from silanized AAO templates.

Table 1. TGA Weight Loss and Onset of Thermal Degradation (T_o) for PC-Infiltrated AAO Templates

	untreated	C^F_8	C^F_{10}	C^H_8	C^H_{10}
weight loss (wt %)	34.1	25.5	30.0	27.2	26.3
T_o (°C)	243	269	266	274	257

From Table 1, the mass of polymer inside the AAO templates was approximated as the percent weight loss measured during TGA. Using this information, DSC data were analyzed to determine the change in heat capacity, glass transition temperature, and glass transition breadth, as marked in Figure 4. In Figure 5(a), the change in heat capacity ΔC_p shows no clear dependence for bulk and PC-infiltrated fluorosilanized AAO templates. However, ΔC_p is slightly higher for PC in alkylsilane-modified AAO templates. This result suggests that bulk and fluorosilane samples have similar fractions of amorphous material undertaking the transition and that alkylsilane samples have a slightly larger fraction.

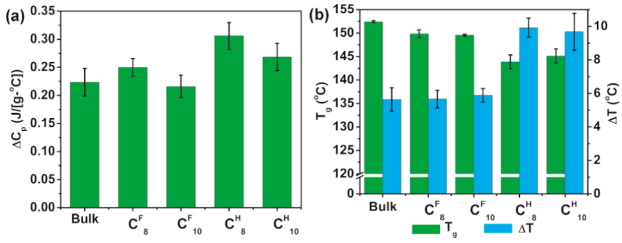

Figure 5. (a) Change in heat capacity (ΔC_p), (b) glass transition temperature (T_g), and breadth (ΔT) for bulk PC and PC melt-wetted into silanized AAO templates. Data are averaged over three samples. ΔC_p is reported based on mass of polymer.

On the other hand, Figure 5(b) shows a reduction in T_g for PC-infiltrated silanized AAO templates as compared to bulk (152.4 ± 0.2 °C). PC-infiltrated alkylsilane-modified AAO templates exhibited the largest reduction in T_g at 144 ± 2 and 145 ± 2 °C for C^H_8 and C^H_{10}. Comparable fluorosilane samples exhibited T_g's of 149.8 ± 0.8 and 149.6 ± 0.2 °C for C^F_8 and C^F_{10}, respectively. Lower T_g values have been previously observed for glass formers inside CPGs[21,31,32] and for poly(methyl methacrylate) inside AAO.[25]

Besides a reduced T_g, the PC-infiltrated alkylsilane-modified AAO templates exhibit a larger transition breadth (ΔT) as compared to bulk and fluorosilane samples. The increased breadth for the alkylsilane samples is consistent with a distribution of microstates sampled by polymer chains and captures the breadth brought about by the secondary features shown in DSC thermograms (Figure 4). This result further supports the idea that the pore's surface influences the nature of PC's glass transition. Additionally, the observed changes in the glass transition could also be due to nonequilibrium chain conformations brought about during the infiltration of the polymer into the nanopore.

It is notable that the chemistry of the silane should have such a varied effect on PC's glass transition. For example, fluorosilanes appeared to have little influence on the nature of the glass transition, except for a slight reduction in the T_g value. On the other hand, the alkyl silane engendered a greater reduction in T_g, an increase in ΔT, and a slight increase in ΔC_p. These differences may be attributed to the various surface energies presented by the silanes, in which the fluorosilane is more hydrophobic than the alkylsilane. It is possible that the coverage of alkyl and fluorosilanes within the AAO nanopore is not equivalent.

In summary, the glass transition of PC inside cylindrical surface-modified AAO nanopores is affected by surface

DOI: 10.1021/mz500725s
ACS Macro Lett. 2015, 4, 151−154

chemistry. As compared to bulk PC, an alkyl surface broadened and reduced the T_g to a greater degree than the fluorinated surface. The length of the silane (8 vs 10 carbons) did not strongly influence the outcome. Without surface modification PC shows evidence of thermal degradation in the presence of the bare AAO surface. Additionally, the tips of the nanowires showed a significant change in the contact angle resulting from the reversal of the nanopore surface from hydrophilic to hydrophobic. These results allow one to isolate the effect of the surface, as there is little free surface available in the cylindrical geometry.

■ ASSOCIATED CONTENT

Supporting Information

Modulated DSC, TGA, and experimental procedure. This material is available free of charge via the Internet at http://pubs.acs.org.

■ AUTHOR INFORMATION

Corresponding Author

*E-mail: jodie.lutkenhaus@che.tamu.edu.

Notes

The authors declare no competing financial interest.

■ ACKNOWLEDGMENTS

This work is supported in part by the American Chemical Society Petroleum Research Foundation (Grant No. 51049-DNI7). We thank the Materials Characterization Facility. We also thank Ms. Kelly Meek and Prof. Yoseff Elabd for GPC testing.

■ REFERENCES

(1) Forrest, J. A.; Dalnoki-Veress, K.; Stevens, J. R.; Dutcher, J. R. *Phys. Rev. Lett.* **1996**, *77*, 2002−2005.
(2) Tate, R. S.; Fryer, D. S.; Pasqualini, S.; Montague, M. F.; de Pablo, J. J.; Nealey, P. F. *J. Chem. Phys.* **2001**, *115*, 9982−9990.
(3) Grimm, S.; Martin, J.; Rodriguez, G.; Fernandez-Gutierrez, M.; Mathwig, K.; Wehrspohn, R. B.; Gosele, U.; San Roman, J.; Mijangos, C.; Steinhart, M. *J. Mater. Chem.* **2010**, *20*, 3171−3177.
(4) Grimm, S.; Giesa, R.; Sklarek, K.; Langner, A.; Gösele, U.; Schmidt, H.-W.; Steinhart, M. *Nano Lett.* **2008**, *8*, 1954−1959.
(5) Chen, B.; Lu, K. *Langmuir* **2011**, *27*, 4117−4125.
(6) Buijnsters, J. G.; Zhong, R.; Tsyntsaru, N.; Celis, J. P. *ACS Appl. Mater. Interfaces* **2013**, *5*, 3224−3233.
(7) Steinle, E. D.; Mitchell, D. T.; Wirtz, M.; Lee, S. B.; Young, V. Y.; Martin, C. R. *Anal. Chem.* **2002**, *74*, 2416−2422.
(8) Popat, K. C.; Mor, G.; Grimes, C. A.; Desai, T. A. *Langmuir* **2004**, *20*, 8035−8041.
(9) Odom, D. J.; Baker, L. A.; Martin, C. R. *J. Phys. Chem. B* **2005**, *109*, 20887−20894.
(10) Ku, A. Y.; Ruud, J. A.; Early, T. A.; Corderman, R. R. *Langmuir* **2006**, *22*, 8277−8280.
(11) Hendren, Z. D.; Brant, J.; Wiesner, M. R. *J. Membr. Sci.* **2009**, *331*, 1−10.
(12) Mark, J. E., 77. Polycarbonate. In *Polymer Data Handbook*, 2nd ed.; Oxford University Press: New York.
(13) Alizadeh, A.; Sohn, S.; Quinn, J.; Marand, H.; Shank, L. C.; Iler, H. D. *Macromolecules* **2001**, *34*, 4066−4078.
(14) Blaszczyk-Lezak, I.; Hernández, M.; Mijangos, C. *Macromolecules* **2013**, *46*, 4995−5002.
(15) Duran, H.; Gitsas, A.; Floudas, G.; Mondeshki, M.; Steinhart, M.; Knoll, W. *Macromolecules* **2009**, *42*, 2881−2885.
(16) Krutyeva, M.; Wischnewski, A.; Monkenbusch, M.; Willner, L.; Maiz, J.; Mijangos, C.; Arbe, A.; Colmenero, J.; Radulescu, A.; Holderer, O.; Ohl, M.; Richter, D. *Phys. Rev. Lett.* **2013**, *110*, 119901.
(17) Serghei, A.; Chen, D.; Lee, D. H.; Russell, T. P. *Soft Matter* **2010**, *6*, 1111−1113.
(18) Koh, Y. P.; Simon, S. L. *J. Phys. Chem. B* **2010**, *114*, 7727−7734.
(19) Koh, Y. P.; Li, Q.; Simon, S. L. *Thermochim. Acta* **2009**, *492*, 45−50.
(20) Li, Q.; Simon, S. L. *Macromolecules* **2009**, *42*, 3573−3579.
(21) Alcoutlabi, M.; McKenna, G. B. *J. Phys.: Condens. Matter* **2005**, *17*, R461−R524.
(22) Jackson, C. L.; McKenna, G. B. *Chem. Mater.* **1996**, *8*, 2128−2137.
(23) Jackson, C. L.; McKenna, G. B. *J. Non-Cryst. Solids* **1991**, *131*, 221−224.
(24) Shin, K.; Obukhov, S.; Chen, J.-T.; Huh, J.; Hwang, Y.; Mok, S.; Dobriyal, P.; Thiyagarajan, P.; Russell, T. P. *Nat. Mater.* **2007**, *6*, 961−965.
(25) Li, L.; Zhou, D.; Huang, D.; Xue, G. *Macromolecules* **2014**, *47*, 297−303.
(26) Li, M.; Wu, H.; Huang, Y.; Su, Z. *Macromolecules* **2012**, *45*, 5196−5200.
(27) Zhang, M.; Dobriyal, P.; Chen, J.-T.; Russell, T. P.; Olmo, J.; Merry, A. *Nano Lett.* **2006**, *6*, 1075−1079.
(28) Jang, W. S.; Jensen, A. T.; Lutkenhaus, J. L. *Macromolecules* **2010**, *43*, 9473−9479.
(29) Eyiler, E.; Chu, I. W.; Rowe, M. D.; Walters, K. B. *J. Appl. Polym. Sci.* **2014**, *131*, n/a−n/a.
(30) Wang, Z.; Cai, N.; Dai, Q.; Li, C.; Hou, D.; Luo, X.; Xue, Y.; Yu, F. *Fibers Polym.* **2014**, *15*, 1406−1413.
(31) Koh, Y. P.; Simon, S. L. *J. Phys. Chem. B* **2012**, *116*, 7754−7761.
(32) Li, X.; Simon, S. L. *Macromolecules* **2008**, *41*, 1310−1317.

DOI: 10.1021/mz500725s
ACS Macro Lett. 2015, 4, 151−154